GSC Biological and Pharmaceutical Sciences

eISSN: 2581-3250 CODEN (USA): GBPSC2

Cross Ref DOI: 10.30574/gscbps

Journal homepage: https://gsconlinepress.com/journals/gscbps/

(RESEARCH ARTICLE)

Check for updates

Binding affinities and molecular dynamics simulations of selected approved drugs and *Mucuna pruriens* phytoconstituents with *Escherichia coli* Shiga toxin

Emmanuel Chuks Oranu [1, *], IC Uzochukwu [4], Ebere Ifejirika Ezeonyi [3], Okonkwo Onyinye Blessing [3], Ejezie Perpetua Chinonyelum [1], RN Egbuna [2] and Chukwubuikem C. Okolo [4]

[1] *Department of Pharmaceutical and Medicinal Chemistry, Faculty of Pharmaceutical Sciences, Chukwuemeka Odumegwu Ojukwu University Igbariam, Igbariam Anambra State, Nigeria.*
[2] *Department of Pharmaceutical Microbiology and Biotechnology, Faculty of Pharmaceutical Sciences, Chukwuemeka Odumegwu Ojukwu University Igbariam, Igbariam Anambra State, Nigeria.*
[3] *Department of Pharmacognosy and Traditional Medicine, Faculty of Pharmaceutical Sciences, Chukwuemeka Odumegwu Ojukwu University Igbariam, Igbariam Anambra State, Nigeria.*
[4] *Department of Pharmaceutical and Medicinal Chemistry, Faculty of Pharmaceutical Sciences, Nnamdi Azikiwe University Awka, Anambra State, Nigeria.*

GSC Biological and Pharmaceutical Sciences, 2025, 30(02), 029–035

Publication history: Received on 18 December 2024; revised on 01 February 2025; accepted on 04 February 2025

Article DOI: https://doi.org/10.30574/gscbps.2025.30.2.0038

Abstract

Shiga toxin (Stx)–producing *Escherichia coli* (STEC), also known as "verocytotoxin- producing *E. coli*" is a major food and waterborne pathogen of zoonotic origin. STEC infection is involved in several life-threatening disease conditions that includes diarrhea, hemorrhagic colitis, and hemolytic-uremic syndrome. We determined the binding affinities of selected approved drugs and *Mucuna pruriens* phytoconstituents to shiga toxin and ricin receptors (a toxin similar in structure to shiga toxin) by molecular docking simulations. The 3D crystal structures of Stx1, Stx2 and ricin receptor were obtained from the protein data bank. The receptors were prepared using PyMol 1.1eval, Chimera 1.10.1 and AutoDock tools vs 1.5.6. The 3D structures of selected approved drugs and *Mucuna pruriens* phytoconstituents were obtained from ZINC and PubChem databases. They were prepared for molecular docking simulations using AutoDock tools vs 1.5.6. Docking protocols were validated by reproducing the PDB crystal structures *in silico*. Molecular docking simulations were executed with a virtual screening script using AutoDockVina 1.1.2 on a Linux platform. Molecular dynamics simulations of two front runner compounds with the reference ligand and protein were done in 1500 ps. Morphine, Butorphanol and riboflavin (phytoconstituent of *Mucuna pruriens*) had binding affinities of -6.6±0.0,-6.4±0.1 and -6.2±0.1 kcal/mol respectively as while the reference ligand, 3-(pyridine-1-ium-1-yl)propane-1-sulfonate had binding affinity of -4.5±0.0kcal/mol. Higher stability were demonstrated by morphine and butorphanol in the molecular dynamics simulations. Morphine, butorphanol and riboflavin are predicted as possible shiga toxin antidotes.

Keywords: Shiga toxin; Molecular docking; Molecular dynamics; Approved drugs; *Escherichia coli*; *Mucuna pruriens*

1. Introduction

Escherichia coli is an important pathogen in animals and humans, and Shiga toxin-producing *Escherichia coli* (STEC) has emerged as important food-borne pathogens, especially serotype O157:H7 (Iweriebor *et al*, 2015). STEC is the etiologic cause of post-diarrheal hemolytic uremic syndrome (HUS), a thrombotic microangiopathy characterized by thrombocytopenia, hemolytic anemia, and acute renal failure following a course of bacterially induced hemorrhagic diarrhoea (Mayer *et al*, 2012). Approximately 5–30% of patients suffer long term morbidity from chronic renal insufficiency, hypertension, or neurological deficits following the resolution of active HUS. Children younger than 2

* Corresponding author: Emmanuel Chuks Oranu.

years of age are particularly susceptible to Shiga toxin-induced HUS, and the overall HUS rates vary between 5–15% of confirmed STEC cases depending on the infecting bacterial strain (Hall *et al*, 2017).

STEC strains are susceptible to antibiotics, but antibiotic therapy is generally contraindicated because antibiotic treatment leads to increased toxin production and risk of HUS development. As a result, the standard of care remains supportive and avoids antibiotics (Iweriebor *et al*, 2015). Diverse strains of microorganism exist in the environment, coupled with the limits of protein detection in environmental samples and this has made it difficult to directly and specifically detect Stx producing microorganisms outside the laboratory (Mauro and Koudelka, 2011).

Stx elicits its action by binding to a specific receptor, globotriaosylceramide (Gb3), on the surface of endothelial cells and toxin internalization by a receptor-mediated endocytic process, followed by toxin interaction with subcellular components that results in protein synthesis inhibition or apoptosis (Karmali, 2004). Binding of Stx to its target cells presumably initiates a complex chain of events, including coagulation and pro- inflammatory processes, that results in HUS. Blocking of Stx binding to endothelial cells to halt these events and prevent the development of HUS might be achieved by generation of specific Stx antibodies by active or passive immunization or by the use of synthetic Gb3 receptor analogues that competitively block toxin binding to the endothelial cell receptor (Basu *et al*, 2016).

The study sought to find possible shiga toxin antidotes from the approved drugs or *Mucuna pruriens* phytoconstituents. Some researchers had earlier demonstrated the venom blocking activities of extracts of *Mucuna pruriens* (Lampariello *et al,* 2012).

2. Methodology

2.1. Preparation of receptors

Bioinformatics mining of the protein data bank (PDB) was done to identify Stx2(4M1U and 1R4P), Stx1(2C5C) and ricin crystal structures(1il4) suitable for the study. The 3D atomic crystal structures of the proteins were obtained from PDB. The proteins were prepared for molecular docking simulations using Chimera 1.10.1 and Auto dock tools 1.5.6. Polar hydrogens and charges were added. The grid spaces were assigned.

2.2. Preparation of ligands

Literature mining was done to identify the phytoconstituents of *Mucuna pruriens*. The electronic structure of the reference ligand, selected approved drugs and phytoconstituents of *Mucuna pruriens* were obtained from ZINC and PubChem database. The ligands were prepared for molecular docking simulations using Autodock tools 1.5.6. Rotatable bonds were assigned, Gesteiger charges were added and then saved as pdbqt files. The prepared proteins and ligands were used for molecular docking simulations.

2.3. Molecular docking

Autodock Vina 1.1.2 was used for molecular docking simulations. The ligands were docked into the receptor to predict their free binding energies using Autodock Vina with the aid of a virtual screening script. Four replicate simulations were done for each of the ligands and the binding affinities reported as mean ± standard deviation. The ligands were ranked based on binding energies and frontrunners selected for molecular dynamics simulations.

2.4. Molecular dynamics

Molecular dynamics simulations were done using GROMACS on Linux platform. The molecular dynamics simulations for three front runner-complexes and for the receptor were implemented.

2.5. Molecular dynamics simulation of protein

The protein was inspected for missing residues, after which GROMACS topology file for the protein was generated. A simulation box for the system was generated after which *in vacuo* energy minimization was done. The system was neutralized appropriately. Energy minimization of the solvated and ionized system was done. Position restrain dynamics was done for 30ps so as to restrain the molecules in a reference position after which molecular dynamics was done for 1500ps and the results analysed.

2.6. Molecular dynamics simulation of protein – ligand complex

In this process a directory was first made for the molecular dynamics simulation and the receptor was examined for missing residues. A .itp file was generated for the protein and ligand from PRODRG server which was used for the simulations. Molecular dynamics simulations were implemented as described above and the results analysed.

3. Results and discussion

The docking was done with three receptors of shiga toxin and one receptor of ricin. The docking results of the three stx receptors. From the result of 4m1u, a stx2 receptor, morphine and butorphanol were the foremost front runners with binding affinities of -6.5±0.0 kcal/mol and -6.2±0.0 kcal/mol respectively above the reference ligand 1PS with binding affinity of -4.5±0.1 kcal/mol. There are several other drugs which had higher binding affinities than the reference ligand as the reference ligand was the 76th ligand after collation as one hundred ligands were used for the docking simulation (Oranu *et al,* 2023). The results of 1R4P, a Stx2 receptor shows that morphine and Apomorphine were the foremost front runner with binding affinities of -6.6±0.0kcal/mol and -6.2±0.0 kcal/mol respectively above the reference ligand 1PS with binding affinity of -4.5±0.0 kcal/mol on the 72nd position. The result of 2c5c, a Stx1 receptor (Boone *et al*, 2016) shows that bedaquiline and propericiazine were the foremost frontrunner with binding affinities of -6.4±0.0 kcal/mol and -6.4±0.0 kcal/mol respectively above the reference ligand dicarbamate with binding affinity of -3.3±0.1 kcal/mol and on the 105th position after collation showing it had lots of frontrunners above it. 2c5c had different drugs used in the docking because it has a different reference ligand which was used for sorting of the drugs or compounds due to the fact that shiga toxin are of two types (Karmali, 2004) and this made it to have different front runners as well.

These drugs having higher binding affinities above their reference ligands can be predicted as possible antidotes of shiga toxin, as high binding affinities above the reference indicates better activity above the reference as well.

In order to further ascertain possible effective result, the receptor of ricin, a toxin similar in structure to shiga toxin (Kulkarni *et al*, 2016) was worked on and the result were collated. Among the results obtained, glimepiride and zafirlukast were the foremost frontrunners with binding affinities of -9.8±0.2 kcal/mol and -9.4±0.0 kcal/mol respectively above their reference ligand 9-Deazeguanine with binding affinity of -6.1±0.0 kcal/mol and on the 91st position.

Another docking shows the result of the front runners of the receptors of shiga toxin against ricin receptor and this was done to know the effect of the front runners on that receptor since ricin is similar to shiga toxin (Roy *et al*, 2018). The front runners as well had higher binding affinity above the reference ligand 9-deazeguanine, making them to be predicted to be more active as one of the reasons for docking against ricin was to know if the front runners of shiga toxin will also be effective against ricin toxin

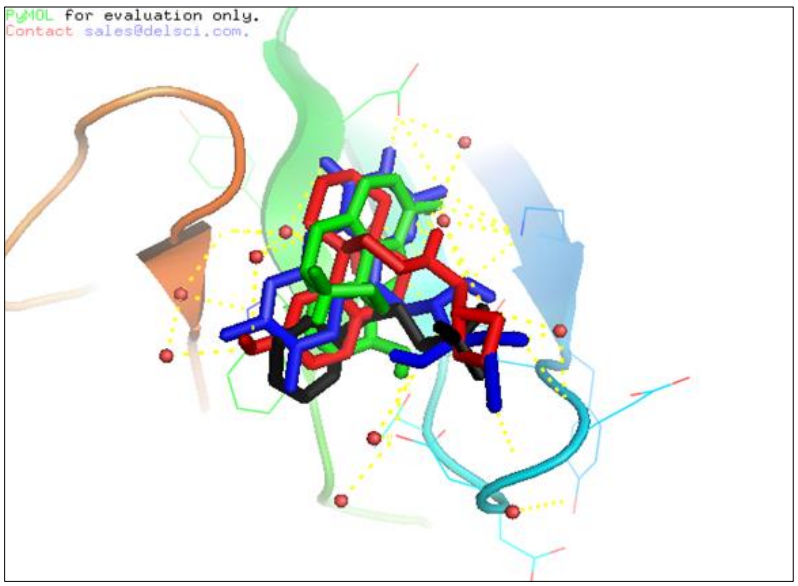

Figure 1 The binding of the front runners (morphine, butorphanol and riboflavin) and reference ligand (1ps) to 4m1u receptor of shiga toxin

The phytoconstituents of *Mucuna pruriens*(an anti-venom) (Meenatchisundaram and Michael, 2010) was also obtained and docked against the receptors of shiga toxin. This had high binding affinities as well and posed front runners which can be potential antidote. Among the front runners obtained, riboflavin was the foremost front runner with binding affinity of -6.2±0.1 kcal/mol for 4m1u receptor, -6.2±0.4 kcal/mol for 1R4P receptor and -5.8±0.2 kcal/mol for 2c5c receptor. It can be seen that riboflavin had more activity against the Stx2 receptor than Stx1 receptor and this is good as stx2 is more virulent than shiga toxin one receptor (Basu *et al*, 2016)

3.1. Molecular Dynamics Results

Results from the trajectories of the production run were analysed and presented below:

3.2. Production run

Different results from the production run were computed from the production run trajectories. The results includes: Stability Profile analysis, radius of gyration and flexibility profile analysis.

3.3. Stability profile analysis

Fig 2 illustrates protein-ligand complex stability and protein stability in terms of RMSD and total energy. The Cα RMSD of the simulated protein over time is a reliable parameter to analyse the stability of the system.

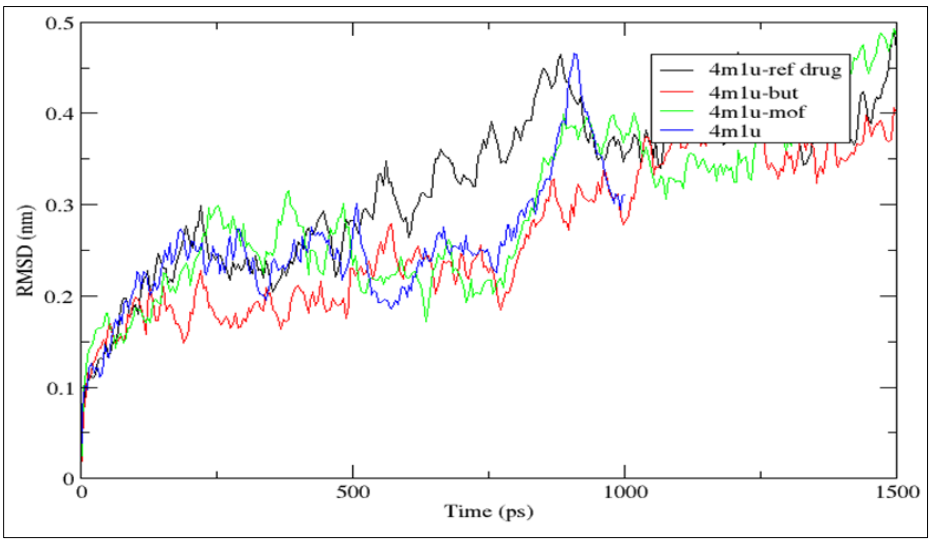

Figure 2 RMSD plot of the molecular dynamic's simulation of the drug target and ligands

From fig 2, it is evident that the first 200ps and 450ps were considered as equilibration phase where slight structural re-organisation occurs for the simulations. The Cα RMSD were averaged over the last 1500ps of the simulation.

In fig 2 having the protein in complex with the ligand, the RMSD of the reference ligand in black colour showed varying degrees of flunctuation between 500ps to 1000ps of the simulation hence showing point of instability (Gooley *et al*, 2005). The RMSD of the protein was more stable than that of the reference ligand. However, the RMSD of morphine in green and butorphanol in red shows higher point of stability than the reference ligand but a few instabilities between 800ps to 1000 ps, notwithstanding all simulations exhibited stable total energy trajectories.

It can be deduced from the graph that butorphanol in red and morphine in green is more stable than the reference ligand and the protein alone.

3.4. Radius of gyration

The radius of gyration measures the structure compactness profile of the ligand and shows various degree of fluctuations (Oranu *et al,*2024). The unstable structure of the reference ligand simulation between 500ps to 1000ps maintained the same degree of compactness throughout the simulation but such was not observed for the other ligands though there were varying compactness. The compacted and unstable structure may be responsible for the flunctuations in the Cα RMSD of the target.

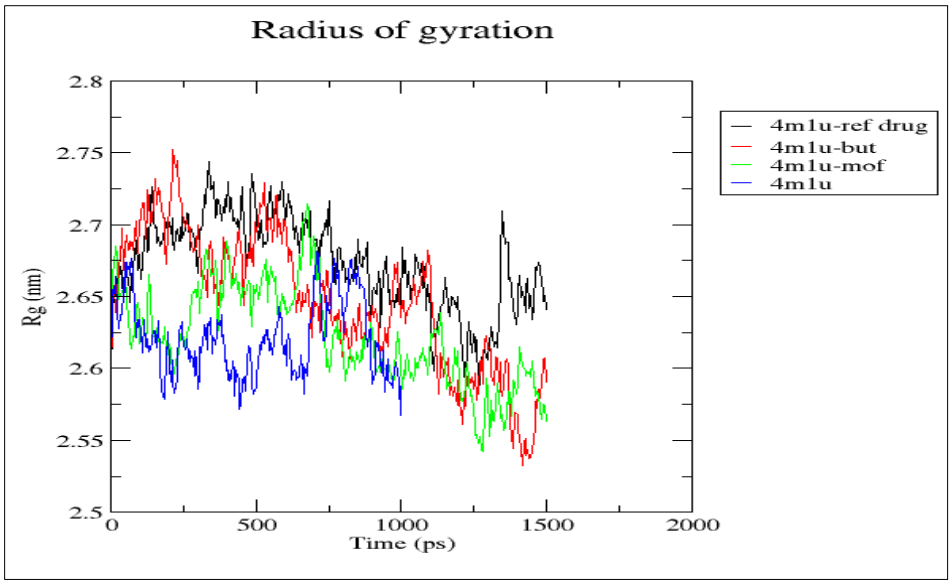

Figure 3 Radius of gyration plot

3.5. Flexibility profile analysis

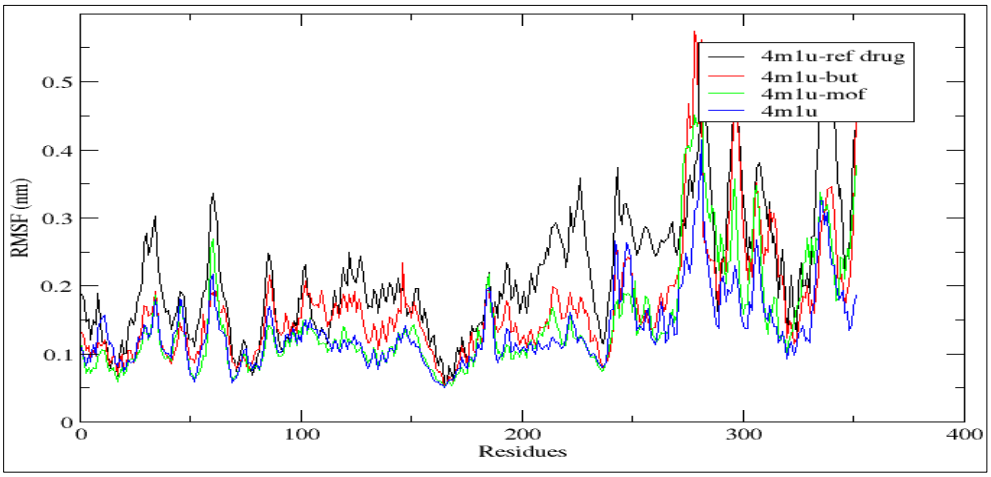

Figure 4 RMSF plot of the molecular dynamics simulation of the drug target and ligands

Residues contributing to complex structural flunctuations can be accessed by root mean square flunctuations (RMSF) of each residue. Analysis of the RMSF shows the amino acid residues involved in the complex and their differences at different residue id (identity) (Gooley *et al*, 2005). Fig 4, shows the functional groups interacting with the residues as well and the type of bond formation involved. It can be seen that there is hydrogen bond formation present in this results showing higher affinity (Martis and Somani, 2005).

It can however be deduced from the result and graphs that morphine and butorphanol are more stable than the reference ligand and can then be said that they are possible antidotes of shiga toxin.

4. Conclusion

Molecular docking simulations of the four receptors gave us front runners which had higher binding affinities than their reference ligand and can be predicted to be shiga toxin antidote. *Mucuna pruriens* phytoconstituents had higher binding affinities and can have anti shiga toxin activity. Molecular dynamics simulation using butorphanol and morphine further showed high stability of these drugs as antidotes of shiga toxin hence the validation. It can then be concluded from this work that morphine, butorphanol, riboflavin from *Mucuna pruriens* and other drugs which have better binding affinity can be predicted as possible shiga toxin antidote.

Compliance with ethical standards

Disclosure of conflict of interest

No conflict of interest to be disclosed.

References

[1] Basu, D., Li, X., Kahn, J. N., May, K. L., Kahn, P. C., & Tumer, E. (2016). The A1 Subunit of Shiga Toxin 2 Has Higher Affinity for Ribosomes and Higher Catalytic Activity than the A1 Subunit of Shiga Toxin 1. Infection and Immunity, 84(1), 149–161. https://doi.org/10.1128/IAI.00994-15.Editor

[2] Boone, J. T., Campbell, D. E., Dandro, A. S., Chen, L., & Herbein, J. F. (2016). A Rapid Immunoassay for Detection of Shiga Toxin-Producing *Escherichia coli* Directly from Human Fecal Samples and Its Performance in Detection of Toxin Subtypes. J Clin Microbiol, 54(12), 3056–3063. https://doi.org/10.1128/JCM.01785-16.Editor

[3] Gooley, P. R., Speed, T. P., & Likic, V. A. (2005). A statistical approach to the interpretation of molecular dynamics simulations of calmodulin equilibrium dynamics. Protein Sciences, 2005(14), 2955–2963. https://doi.org/10.1110/ps.051681605.with

[4] Hall, G., Kurosawa, S., & Stearns-kurosawa, D. J. (2017). Shiga Toxin Therapeutics : Beyond Neutralization. Toxins, 291(9), 1–1. https://doi.org/10.3390/toxins9090291

[5] Hoffer, L., Chira, C., Marcou, G., Varnek, A., & Horvath, D. (2015). SAMPLE—Sampler for Multiple Protein-Ligand Entities: Methodology and Rigid-Site Docking Benchmarking. Molecules, 2015(20), 8997–9028. https://doi.org/10.3390/molecules20058997

[6] Iweriebor, B. C., Iwu, C. J., Obi, L. C., Nwodo, U. U., Okoh, A. I., & Etal. (2015). Multiple antibiotic resistances among Shiga toxin producing *Escherichia coli* O157 in feces of dairy cattle farms in Eastern Cape of South Africa. BMC Microbiology, 15(213), 1–9. https://doi.org/10.1186/s12866-015-0553-y

[7] Karmali, M. A. (2004). Prospects for Preventing Serious Systemic Toxemic Complications of Shiga Toxin – Producing *Escherichia coli* Infections Using Shiga Toxin Receptor Analogues. Editorial Commentary, 189(1), 355–359.

[8] Kulkarni, J. L., Mulye, M. S., Tolani, S. R., & Yadav, M. (2016). Biochemical Aspects of Ricin-Ribosome Complex : A Short Review. Research Journal of Biology, 4(4), 29–37.

[9] Lampariello, L. R., Cortelazzo, A., Guerranti, R., Sticozzi, C., & Valacchi, G. (2012). The Magic Velvet Bean of *Mucuna pruriens*. Journal of Traditional and Complementary Medicine, 2(4), 331–339. https://doi.org/10.1016/S2225-4110(16)30119-5

[10] Martis, E. A., & Somani, R. R. (2005). Drug Designing , Discovery and Development Techniques. Retrieved from www.intechopen.com

[11] Mauro, S. A., & Koudelka, G. B. (2011). Shiga Toxin: Expression, Distribution, and Its Role in the Environment. Toxins, 2011(3), 608–625. https://doi.org/10.3390/toxins3060608

[12] Mayer, C. L., Leibowitz, C. S., Kurosawa, S., & Stearns-kurosawa, D. J. (2012). Shiga Toxins and the Pathophysiology of Hemolytic Uremic Syndrome in Humans and Animals. Toxins, 2012(4), 1261–1287. https://doi.org/10.3390/toxins4111261

[13] Meenatchisundaram, S., & Michael, A. (2010). Antitoxin activity of *Mucuna pruriens* aqueous extracts against Cobra and Krait venom by in vivo and in vitro methods. Internatonal Journal of Pharmtech Research, 2(1), 870–874.

[14] Oranu E.C, Adanna I, Egbuna R.N, Ebere I. E, Okolo C.C, Uzochukwu I. C. (2023). Previous and potential mutations of Sars-cov-2 receptors and their interaction with known inhibitors. GSC Biological and Pharmaceutical Sciences, 24(3), 234-246.

[15] Oranu E. C, Esther O. E, Adanna I., Obidimma C.O, Belinda C. U, Perpetua C. E, Uzochukwu I.C. (2024). Validation of the binding affinities and stabilities of ivermectin and moxidectin against Sars-CoV-2 receptors using molecular docking and molecular dynamics simulation. GSC Biological and Pharmaceutical Sciences, 26(1), 303-314.

[16] Roy, C. J., Ehrbar, D. J., Bohorova, N., Bohorov, O., & Kim, D. (2018). A Humanized Monoclonal Antibody against the Enzymatic Subunit of Ricin Toxin Rescues Rhesus macaques from the Lethality of Aerosolized Ricin, september(6), 1–27.

[17] Trott O., Olson A. J., AutoDock Vina: improving the speed and accuracy of docking with a new scoring function, efficient optimization and multithreading, Journal of Computational Chemistry 31 (2010). 455-461..